Quantum satellites and tests of relativity

Matteo Schiavon, Giuseppe Vallone, Francesco Vedovato and Paolo Villoresi

Dipartimento di Ingegneria dell'Informazione, Università degli Studi di Padova, Padova 35131, Italy

Istituto Nazionale di Fisica Nucleare (INFN) — Sezione di Padova, Italy

Piergiovanni Magnani

Department of Physics, Politecnico di Milano, Milano 20133, Italy

Alexander R. H. Smith

Department of Physics and Astronomy, Dartmouth College, Hanover, New Hampshire 03755, USA

Sai Vinjanampathy

Department of Physics, Indian Institute of Technology-Bombay, Powai, Mumbai 400076, India

Centre for Quantum Technologies, National University of Singapore, 3 Science Drive 2, 117543 Singapore, Singapore

Daniel R. Terno*

Department of Physics and Astronomy, Macquarie University, Sydney, NSW 2109, Australia
E-mail: daniel.terno@mq.edu.au

Deployment of quantum technology in space provides opportunities for new types of precision tests of gravity. On the other hand, the operational demands of such technology can make previously unimportant effects practically relevant. We describe a novel optical interferometric red-shift measurement and a measurement scheme designed to witness the possible spin-gravity coupling effects.

Keywords: Equivalence principle; satellite-based experiments; optics; spin.

1. Introduction

Amazing progress in quantum sensing and quantum, together with satellite deployment of quantum technologies have ushered in a new era of experimental physics in outer space. The success of the first space based quantum key distribution experiments performed with the Micius satellite[1], is expected to be soon followed by European and North American missions. Current missions, such as LAGEOS-2, BEACON-C and LCT on Alphasat I-XL, are adapted for quantum optics experiments[2,3]. While the primary goal of the space-based platforms is to provide links for global quantum key distribution, the missions also envisage substantial scientific programs. These experiments have the exciting potential to enable novel searches for signatures of quantum gravity and/or physics beyond the standard model[4].

Here we describe the interplay of these technologies with the Einstein Equivalence Principle (EEP). The principle comprises three statements[5,6]. The first — *Weak Equivalence Principle* (WEP) — states that the trajectory of a freely falling test body is independent of its internal composition. Closely related to the WEP

is the Einstein elevator: if all bodies fall with the same acceleration in an external gravitational field, then to an observer in a small freely falling lab in the same gravitational field, they appear unaccelerated[6]. The remaining two statements deal with outcomes of non-gravitational experiments performed in freely falling laboratories where self-gravitational effects are negligible. The second statement — *Local Lorentz Invariance* — asserts that such experiments are independent of the velocity of the laboratory where the experiment takes place. The third statement — *Local Position Invariance* (LPI) — asserts that "the outcome of any local non-gravitational experiment is independent of where and when in the universe it is performed"[5].

We consider a novel all-optical test of LPI and the inertial and aspects of the spin-gravity coupling, commenting on implications for the validity of the WEP.

2. Optical test of position invariance

Tests of the "when" part of the LPI bound the variability of the non-gravitational constants over cosmological time scales[7]. The "where" part was expressed in Einstein's analysis of what in modern terms is a comparison of two identical frequency standards in two different locations in a static gravitational field. The so-called *red-shift* implied by the LPI affects the locally measured frequencies of a spectral line that is emitted at location 1 with ω_{11} and then detected at location 2 with ω_{12}. The red-shift can be parametrized at the leading post-Newtonian order as

$$\Delta\omega/\omega_{11} = (1+\alpha)(U_2 - U_1) + \mathcal{O}(c^{-3}), \tag{1}$$

where $\Delta\omega := \omega_{12} - \omega_{11}$, $U_i := -\phi_i/c^2$ has the opposite sign of the Newtonian gravitational potential ϕ_i at the emission (1) and detection (2), while $\alpha \neq 0$ accounts for possible violations of LPI. In principle, α may depend on the nature of the clock that is used to measure the red-shift[5]. The standard model extension includes variously constrained parameters that predict LPI violation[8,9]. Alternative theories of gravity not ruled out by current data also predict $\alpha \neq 0$[5,10].

A typical red-shift experiment involves a pair of clocks, naturally occurring[11] or specially-designed[12–14], whose readings are communicated by electromagnetic (EM) radiation. The resulting estimates of α are based on comparison of fermion-based standards. Hence, different types of experiments, which employ a single EM-source and compare optical phase differences between beams of light traversing different paths in a gravitational field, provide a complementary test of LPI.

Such an all-optical experiment was proposed as a possible component of the QEYSSAT mission[4]. A photon time-bin superposition is sent from a ground station on Earth to a spacecraft, both equipped with an interferometer of imbalance l, in order to temporally recombine the two time-bins and obtain an interference pattern depending on the gravitational phase-shift:

$$\varphi_{\rm gr} = \frac{\Delta\omega}{\omega}\frac{2\pi}{\lambda}l \approx (1+\alpha)\frac{2\pi}{\lambda}\frac{ghl}{c^2}\ , \tag{2}$$

where g is the Earth's gravity, h the satellite altitude and $\lambda = 2\pi c/\omega$ the sent wavelength. For $\alpha = 0$, the order of magnitude of the gravitational red-shift is about 1 rad supposing $\lambda = 1550$ nm, l=1.2 km and an altitude $h = 1500$ km (which corresponds to $\Delta U \approx -1.3 \times 10^{-10}$).

However, a careful analysis of this optical COW-like experiment[15] revealed that first-order Doppler effects are roughly 10^5 times stronger than the desired signal $\varphi_{\rm gr}$ from which α would be estimated. This first-order Doppler effect is an unavoidable part of the interferometric phase[16] was recently measured by exploiting large-distance precision interferometry along space channels[17], which constitute a resource for performing fundamental tests of quantum mechanics in space and space-based quantum cryptography.

We propose[18] a new gravitational red-shift experiment, which uses a single EM-source and a double large-distance interferometric measurement performed at two different gravitational potentials. By comparing the phase-shifts obtained at a satellite and on Earth, it is possible to cancle the first-order Doppler effect. Thus, this experimental proposal allows for a bound on α quantifying the violation of LPI in the EM-sector with a precision on the order of 10^{-5}.

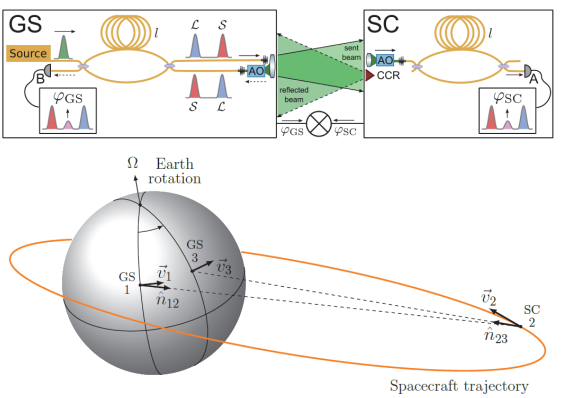

Fig. 1. Top: A schematic diagram of the proposed experiment. Both the ground station (GS) and spacecraft (SC) are equipped with a MZI of equal delay line l and an adaptive optics system for fibre injection. Bottom: The geometry of the GS and SC used in the experiment, where $\vec{v}_1$ is the velocity of the GS at the emission location and potential U_1; $\vec{v}_2$ is the velocity of the SC at the detection location on the satellite and potential U_2; $\vec{v}_3$ is the velocity of the ground station at the detection of the beam retro-reflected by the SC, which occurs at a potential $U_3 = U_1$.

This proposal[17] is comprised of an interferometric measurement obtained by sending a light pulse through a cascade of two fiber-based Mach-Zehnder interferometers (MZI) of equal temporal imbalance τ_l. After the first MZI, the pulse is split into two temporal modes, called *short* ($\mathcal{S}$) and *long* ($\mathcal{L}$) depending on the path taken in the first MZI. The equal imbalance of the two MZIs guarantees that the two pulses are recombined at the output of the second MZI, where they are detected. Such a satellite interferometry experiment setup is sketched in Fig. 1.

The combination of the possible paths the pulses may take leads to a characteristic detection pattern comprised of three possible arrival times for each pulse, as depicted in the insets of the upper picture in Fig. 1. The first (third) peak corresponds to the pulses that took the $\mathcal{S}$ ($\mathcal{L}$) path in both the MZIs, while the mid peak is due to the pulse that took the $\mathcal{S}$ path in the first interferometer and the $\mathcal{L}$ path in the second interferometer, or vice versa. Hence, interference is expected only in the central peak due to the indistinguishability of these latter two possibilities. A successful realization of the experiment depends on a number of important technical aspects that are described in detail in Ref. 18.

A bound on α is retrieved from the difference of the two phase-shifts, $\varphi_{\rm SC}$ and $\varphi_{\rm GS}$, that are obtained from interferometric measurements on the spacecraft and ground station, respectively. As just described, the interfering beams take different paths in the passage through the two MZIs. At the satellite, the beam that took the $\mathcal{L}$ path on Earth and the $\mathcal{S}$ path on the spacecraft interferes with the beam that passed took the $\mathcal{S}$ path on Earth and then took the $\mathcal{L}$ one on the spacecraft. This interference is a result of the phase difference $\varphi_{\rm SC}$. Analogously, at the ground station (GS) the beams that were delayed on the Earth before and after their round trip to the spacecraft (SC) will also interfere because of the phase difference $\varphi_{\rm GS}$.

The first-order Doppler terms are eliminated by manipulating the corresponding data sets from the GS and SC in a manner similar to the time-delay interferometry techniques[19] and those used in the Gravity Probe A experiment[13]. The basis for the derivation is the observation[16,18] that the phase difference at each detector is proportional to the proper time difference at the emission, that is related to the different travel times over $\mathcal{S}$ and $\mathcal{L}$. The key feature allowing for this elimination is that the ratio of the terms stemming from the first-order Doppler effect the two signals, $\varphi_{\rm SC}$ and $\varphi_{\rm GS}$ is exactly two[18]. Hence the target signal is $S = \varphi_{\rm SC} - \frac{1}{2}\varphi_{\rm GS}$, leading to

$$\frac{S}{\omega_0 \tau_l} = (1+\alpha)(U_2 - U_1) + \tfrac{1}{2}(\beta_2^2 - \beta_1^2) - \vec{\beta}_1 \cdot (\vec{\beta}_1 - \vec{\beta}_2) - (\mathfrak{d}_2^2 - \mathfrak{d}_1^2) - T(\hat{n}_{12} \cdot \vec{a}_1) - \left((\vec{\beta}_2 - \vec{\beta}_1)^2 - (\mathfrak{d}_2 - \mathfrak{d}_1)^2\right) \frac{\tau_l}{4T}, \qquad (3)$$

where α parameterizes the violation of LPI, $\vec{\beta}_i := \vec{v}_i/c$, $\mathfrak{d}_i := \hat{n}_{12} \cdot \vec{\beta}_i$, T is the zeroth order time-of-flight between the GS and the SC, $\vec{a}_1$ is the centripetal acceleration of the GS at 1.

3. Weak equivalence principle and orbiting clocks

Matter of the Standard Model is characterized by two parameters of the irreducible representations of the Poincaré group: mass and spin (or helicity). General relativity is a universal interaction theory about masses[20], as the Newtonian gravity is, with polarization effects implicitly omitted from the WEP.

Regardless of their origins, spin-gravity coupling terms provide effective corrections to the Hamiltonian in the limit of weak gravity and non-relativistic motion.

The leading terms of the Hamiltonian of a free spin-$\frac{1}{2}$ particle that take into account the effects of rotation of the reference frame with angular velocity $\vec{\omega}$ and acceleration $\vec{a}$ (or a uniform gravitational field) can be represented as

$$H = H_{\rm cl} + H_{\rm rel} + H_\sigma + H_{\rm ext}. \tag{4}$$

The first three terms on the right hand side are obtained by performing the standard Foldy-Wouthuysen transformation and taking the non-relativistic limit [21]. The term $H_{\rm cl}$ represents the standard Hamiltonian of a free non-relativisitc particle in a non-inertial frame, $H_{\rm rel}$ describes the higher-order relativistic corrections that do not involve spin, and

$$H_\sigma = -\tfrac{1}{2}\hbar\vec{\omega}\cdot\vec{\sigma} + \frac{\hbar}{4mc^2}\vec{\sigma}\cdot(\vec{a}\times\vec{p}). \tag{5}$$

Finally, the term

$$H_{\rm ext} = \frac{\hbar k}{2c}\vec{a}\cdot\vec{\sigma} \tag{6}$$

represents the spin-accelerating (or spin-gravity) coupling. It is a limiting form of the simplest phenomenological addition to the Dirac equation that breaks the WEP [22]. For the value $k = 1$ it results from a particular version of the Foldy-Wouthuysen transformation [23]. While commonly considered a mathematical artefact of this transformation, the term naturally arises in gravitationally inspired Standard Model extensions. Only model-dependent bounds on k in $H_{\rm ext}$ were obtained by a variety of techniques [24], including the optical magnetometery [25].

The spin dependent terms are small under normal conditions. On the Earth's surface $\hbar g/c = 2.15\times10^{-23}$ eV, which is equivalent to an effective magnetic field of 3.7×10^{-19} Tl, still several orders of magnitude below the peak sensitivity of optical magnetometery. The spin-rotation term is significantly larger, since already on the ground $\omega c/g = 2.22\times10^{3}$. It will be about an order of magnitude stronger for low-orbit satellites that are planned to carry entangled optical clocks aiming to establish the precision of $10^{-18}-10^{-20}$, making it a factor to consider in the clock design.

A potentially promising way of detecting these effects is via so-called weak amplification [26]. Weak value amplification involves two systems (typically referred to as "system" and "meter") that can interact via an interaction Hamiltonian of the form $q\delta(t-t_0)\hat{A}\otimes\hat{p}$. The bipartite system-meter is prepared in an initial state $|s_i\rangle\otimes|m_i\rangle$, following which the two are allowed to interact for a small time that includes t_0. Following this, the system is measured and measurements corresponding to a post-selected system state $|s_f\rangle$ are considered. This pre- and post-selection induces a "kick" in the meter state, given by the evolution $e^{-iq\mathcal{A}_w\hat{p}}|m_i\rangle$, where $\mathcal{A}_w \equiv \langle S_f|A_s|S_i\rangle/\langle S_f|S_i\rangle$.

The key insight here is that since $\langle S_f|S_i\rangle$ can be a small number, the measurement of q is influenced by a large multiplicative factor $\mathcal{A}_w$. A subsequent measurement of the meter reveals the desired parameter q. Trapped atoms are potentially promising system to implement this scheme [26].

The simplest model of such a set-up consists of a species of spin interacting with a harmonic mode, subject to an interaction of the form

$$H \approx \hbar\omega_t(a^\dagger a + 1/2) + \frac{\hbar\omega_g}{2}\sigma_z + \hbar\lambda[(1 - i\delta)\sigma_+ a + (1 + i\delta)\sigma_- a^\dagger], \tag{7}$$

ω_g being the gravitational term and constants δ, λ are related to the interaction with the harmonic mode[26]. Analysis of the unitary evolution that is followed by post-selection indicates that for realistic parameter values the inertial and gravitational effects are within the sensitivity range of the optical magnetometery.

References

1. J. Yin *et al.*, *Science* **356**, 1140 (2017).
2. G. Vallone *et al.*, *Phys. Rev. Lett.* **116**, 253601 (2016).
3. K. Günthner *et al.*, `arXiv:1608.03511` (2016).
4. A. Rideout *et al.*, *Class. Quant. Grav.* **29**, 224011 (2012).
5. C. M. Will, *Living Rev. Relativity* **17**, 4 (2014).
6. E. Poisson and C. W. Will, *Gravity: Newtonian, Post-Newtonian, Relativistic*, (Cambridge University Press, 2014).
7. J.-P. Uzan, *Living Rev. Relativity* **14**, 2 (2011).
8. V. A. Kostelecký and N. Russell, *Rev. Mod. Phys.* **83**, 11 (2011).
9. S. Liberatti, *Class. Quantum Grav.* **30**, 133001 (2013).
10. J. Sakstein, *Phys. Rev. D* **97**, 064028 (2018).
11. J. C. LoPresto, C. Schrader, and A. K. Pierce, *Astrophys. J* **376**, 757 (1991).
12. R. V. Pound and G. A. Rebka, Jr., *Phys. Rev. Lett.* **4**, 337 (1960).
13. R. F. C. Vessot *et al.*, *Phys. Rev. Lett.* **45**, 2081 (1980).
14. N. Ashby, T. E. Paker, and B. R. Patla, *Nature Phys.* **14**, 822-826 (2018).
15. A. Brodutch *et al.*, *Phys. Rev. D* **91**, 064041 (2015).
16. D. R. Terno, G. Vallone, F. Vedovato and P. Villoresi, *Phys. Rev. D* **101**, 104052 (2020).
17. G. Vallone *et al.*, *Phys. Rev. Lett.* **116**, 253601 (2016).
18. D. R. Terno, F. Vedovato *et al.*, `arXiv:1811.04835` (2018).
19. M. Tinto and S. V. Dhurandhar, *Living Rev. Relativity* **17**, 6 (2014).
20. W.-T. Ni, *Rep. Prog. Phys.* **73**, 056901 (2010).
21. F. W. Hehl and W.-T. Ni, Phys. Rev. D **42**, 20145 (1990).
22. A. Peres, *Phys. Rev. D* **18**, 2739 (1978).
23. Y. N. Obukhov, *Phys. Rev. Lett.* **86**, 192 (2001).
24. M. S. Safronova *et al.*, *Rev. Mod. Phys.* **90** 025008 (2018).
25. D. F. J. Kimball *et al.*, *Ann. Phys. (Berlin)* **525**, 514 (2013).
26. S. Ghosh, L.-C. Kwek, D. R. Terno, and S. Vinjanampathy, `arXiv:1912.10693` (2019).